Use of Fiber Bragg Grating Sensors for the characterization of deformation of composites structures

- LLR demonstrator -

LLR Ecole Polytechnique
F - 91128 PALAISEAU Cedex

Marc Anduze *(LLR)*

Framework (1/2)

<u>Project :</u> Electromagnetic calorimeter (ECAL) for ILC

Designing a suitable calorimeter for physics of the International Linear Collider.

The best approach is expected to be able to individually recognize each particle of an event (PFLOW)

High Density, compactness and granularity of this calorimeter with minimum dead zones : ECAL W/Si

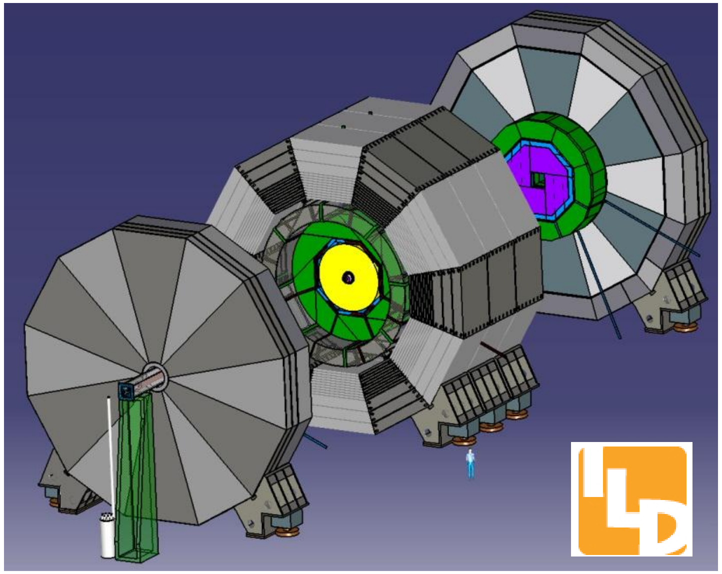

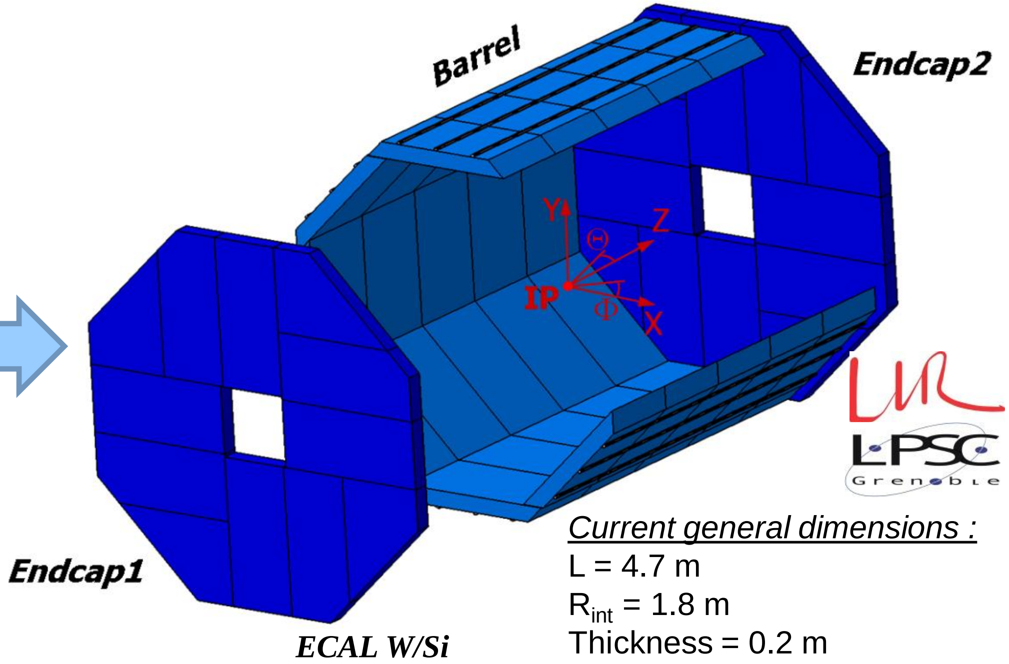

<u>Current general dimensions :</u>

L = 4.7 m

R_{int} = 1.8 m

Thickness = 0.2 m

Framework (2/2)

Concept of self-supporting alveolar structure made of composite material (C/E), including half of the absorber (W) and wherein the detector elements are inserted (Si)

Example : barrel module (~2 tons)

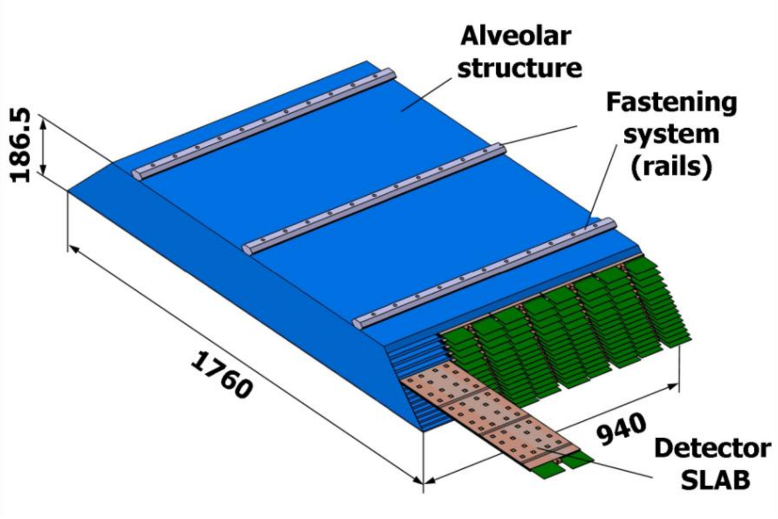

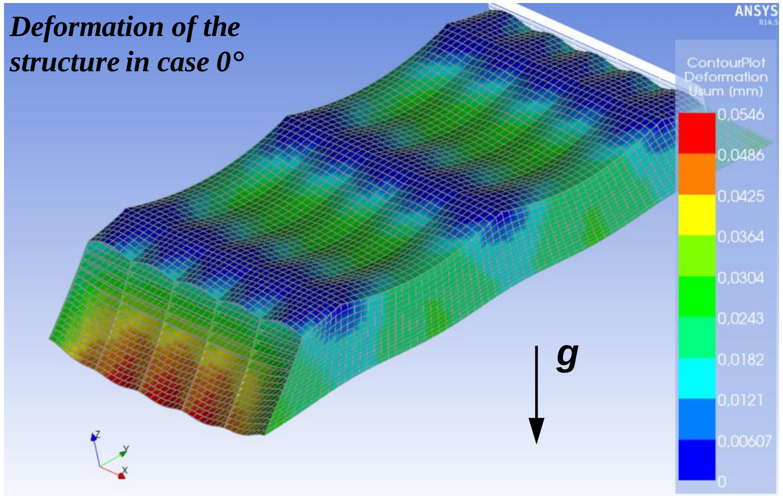

max stress
need to equip a prototype with sensors in these zones to verify and validate the simulations

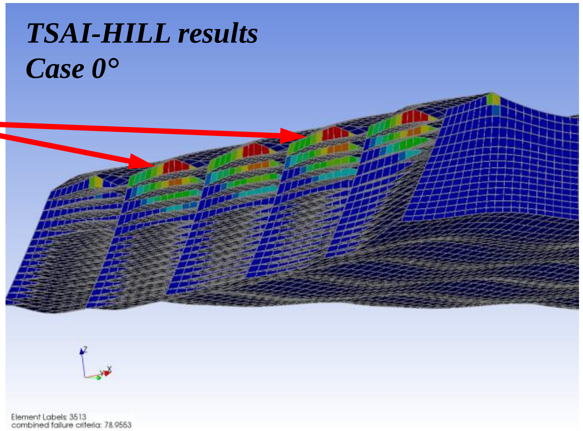

Choice of sensor

Specifications:

1) Measure the **stress** in inter-cells walls : **Strain gauge** (measure of relative elongation)

2) Sensors under the fastening system (rails): **small size** and **easy to place** them at the center of the structure (~ 1.5 m)

3) Sensors included directly during the manufacturing step?
Non-invasive sensors concept : do not disturb the mechanical behaviour of each layer of composite and support the curing conditions
(temperature: 120 ° C, pressure: 7 bar)

4) **Large number** of sensors along each wall

→ Optical fiber with Bragg grating sensors

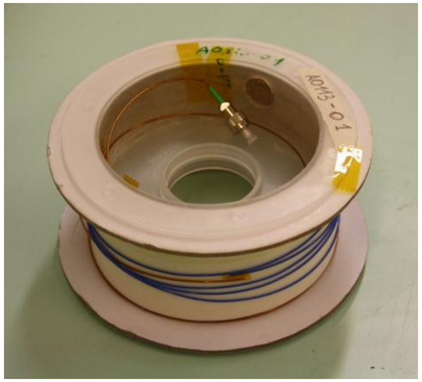

Principle of Bragg grating (1/3)

Definition: A Fiber Bragg Grating (FBG) is a periodic perturbation of the refractive index along the fiber length (obstacles) which is formed by exposure of the core to an intense optical interference pattern (ex: UV irradiation)

Etching process by UV irradiation

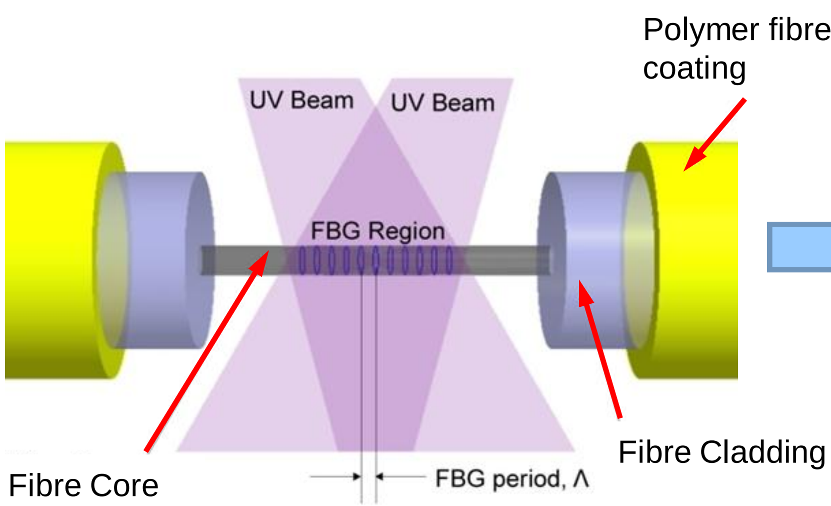

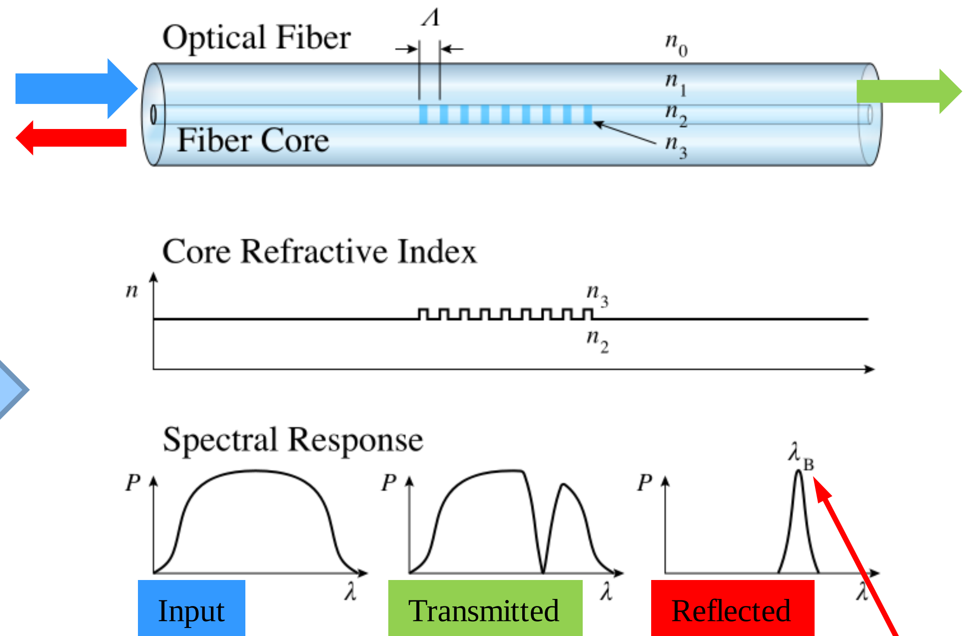

reflectivity spectrum, Bragg wavelength:

$$\lambda_B = 2\Lambda\, n_{eff}$$

with Λ: grating period fringes
n_{eff} : effective refractive index of the core

Principle of Bragg grating (2/3)

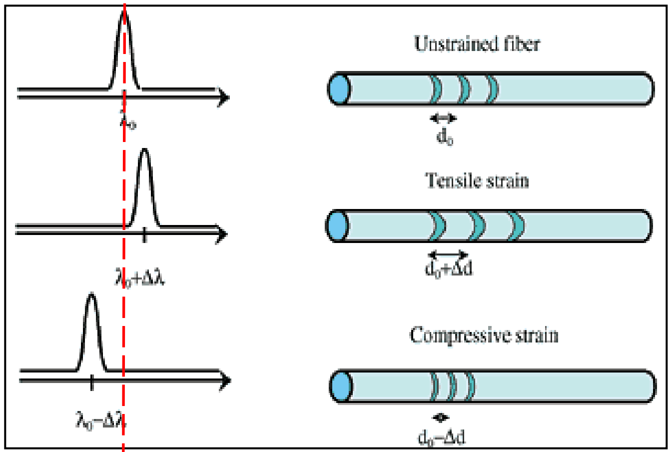

Use as a Strain Gauge: Under external solicitations (temperature **T**, strain **ε,** pressure ...) the effective refractive index (n_{eff}) and the grating period (Λ) change.

The Bragg wavelength value increases or decreases according to a compressive or tensile effect :

$$\frac{\Delta\lambda_b}{\lambda_b} = a\Delta T + b\varepsilon$$

with : a~7 10^{-6} /°C ; b~0,78 10^{-6} /µm/m (single mode standard fibers : SMF 28)

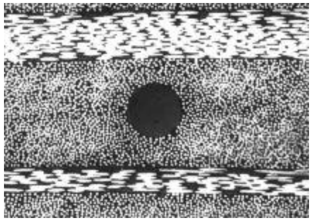

minimally invasive sensor

Inherent advantages of optical fiber:

- High temperature resistance (-70° à 400°C)
- Optical signal : high dynamic range and immunity to electromagnetic interference, high voltages, vibrations …
- Small size and weight which facilitate their integration in the composite
- Absolute and narrow spectral signature: multiplexing capability and no calibrations

Principle of Bragg grating (3/3)

Technological obstacles:

- Fragility
- Problems of connectivity
- Handling instrumented parts
- Machinability & reparability
- Quality of the interface material/fiber
- Residual stress due to manufacturing process (three-dimensional effects of curing process)
- Cost of sensors and interrogation units

Si720 : Optical Spectrum Analyzer (Micron Optics)
Si425 : FBG Interrogator (to record FBG peak wavelengths as a function of time)

Applications of FBG :

- Telecommunications: passive filtering components
- Engineering:
  Monitoring deformations of bridges,
  Integration into the wind turbine blades
- Health Monitoring of structures :
  Detection of damages
  (cracks, impacts, delamination ...)

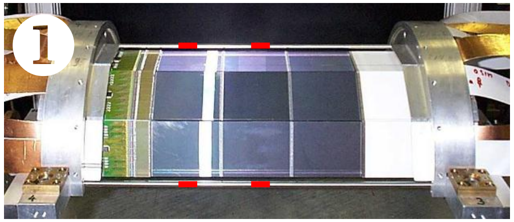

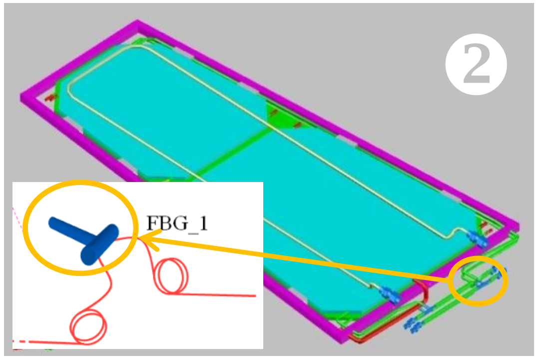

① Monitoring deformations of vertex detector
② monitoring RPC gas temperature (INFN-Frascati)

LLR demonstrator

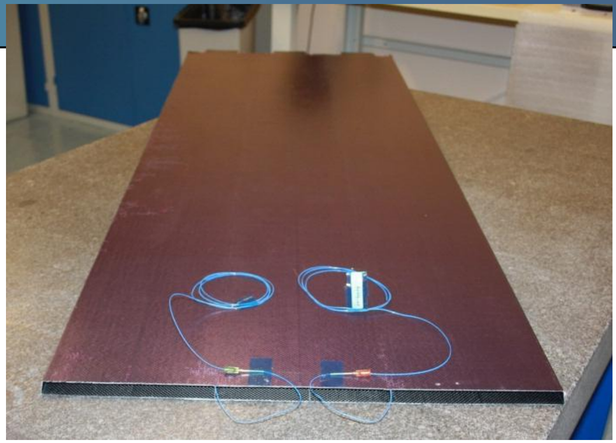

Bending tests (3 and 4) on demonstrator equipped with 5 FBGs per fiber

<u>Choice of demonstrator:</u>

1) A representative monolayer structure (3 cells)

2) implementation of FBG in the most stressed areas (directly under the rails: FBG1/FBG3/FBG5) + area with high elongation (FBG2/FBG4).

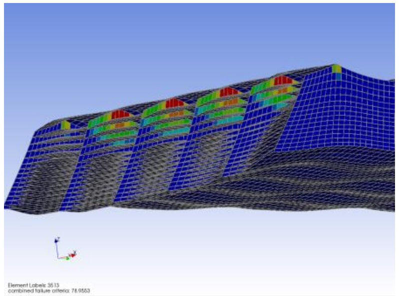

Positioning of FBGs based on simulations

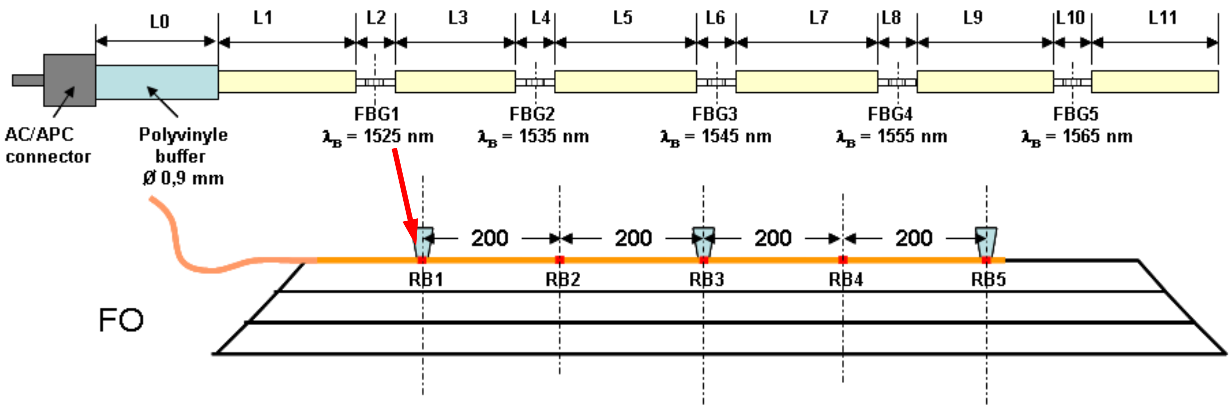

3) Optical fibers directly embedded into inter-cell walls, during the manufacture of the demonstrator

Implementation

Integration of the fibers during the draping steps of the laminate:

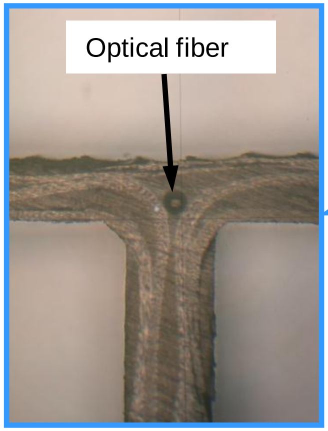

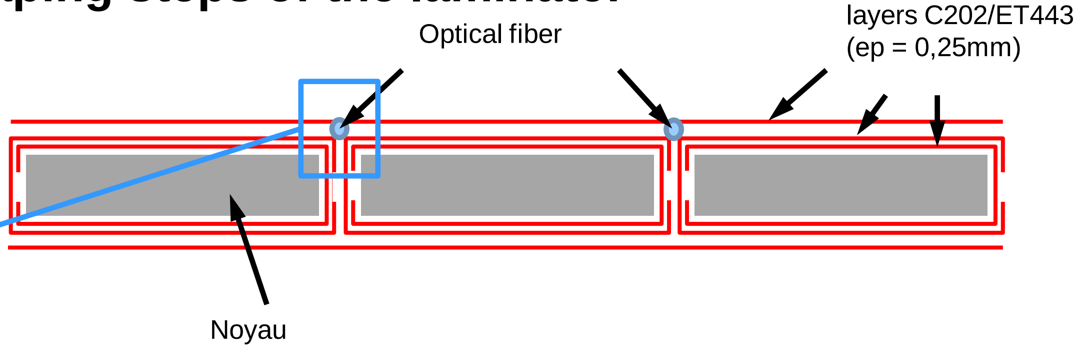

Manual placement of a fiber

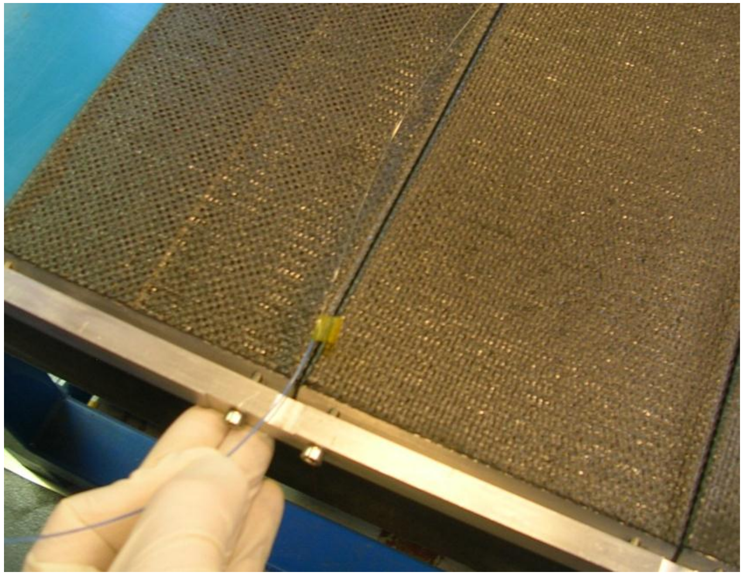

<u>Delicate operations:</u>

1) manipulation of an optical fiber with weak zones: no protection (cladding + coating) around the FBG to optimize the fiber/composite interface
2) risks of pinching the fiber during the draping
3) risks of rupture during cooking process caused by internal strength imposed by autoclave
1) FBG positioning errors estimated : ± 1 mm

Checks before/after curing (1/2)

1st example of spectrum response (@ 23°C) :

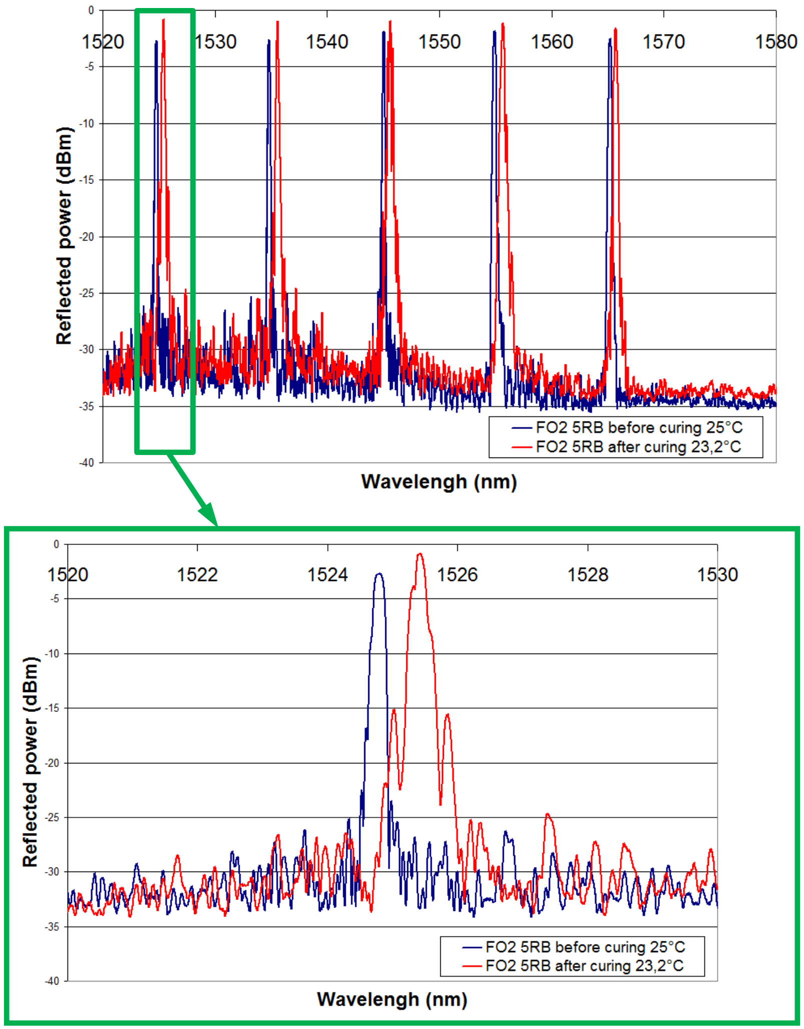

λ_B intended (nm)	λ_B before curing (nm)	λ_B after curing (nm)	$\Delta\lambda_B$ (nm)
1525	1524,81	1525,45	+0,64
1535	1534,86	1535,61	+0,75
1545	1545,1	1545,67	+0,57
1555	1554,96	1555,72	+0,76
1565	1565,25	1665,75	+0,5

Operational optical fiber but:

- systematic shift of λ_B
- Changes almost identical for all FBGs

certainly the result of thermomechanical stresses caused by process (pressure, expansion due to temperature ...)

Checks before/after curing (2/2)

2nd example of spectrum response (@ 23°C) :

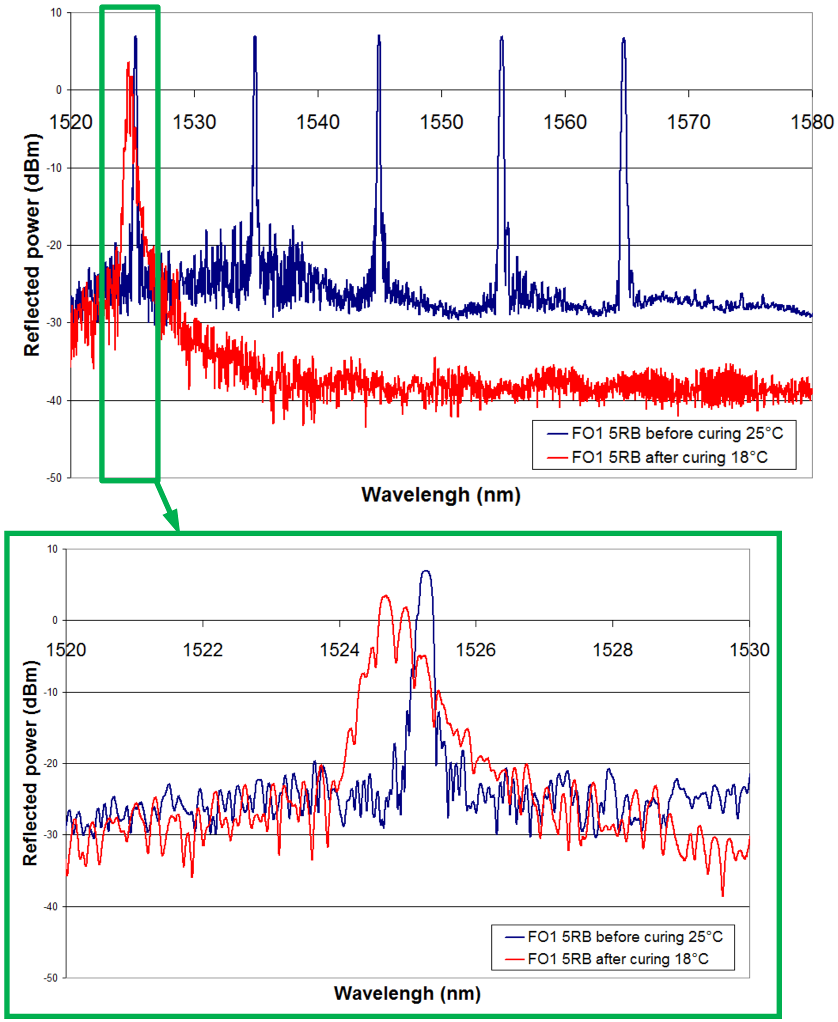

λ_B intended (nm)	λ_B before curing (nm)	λ_B after curing (nm)	$\Delta\lambda_B$ (nm)
1525	1525,31	1524,71	-0,6
1535	1534,66	-	-
1545	1545	-	-
1555	1554,94	-	-
1565	1564,8	-	-

Nonoperational optical fiber:
only the first λ_B is OK (FBG1)
certainly broken between FBG1 and FBG2

Setup

Description:

- 3 and 4 bending setup
- Non-destructive tests
- Loads limited to obtain central deflection <5 mm (hyp of wide displacements)
- Design of a specific setup

(dimensions are not adapted to a tensile testing machine)

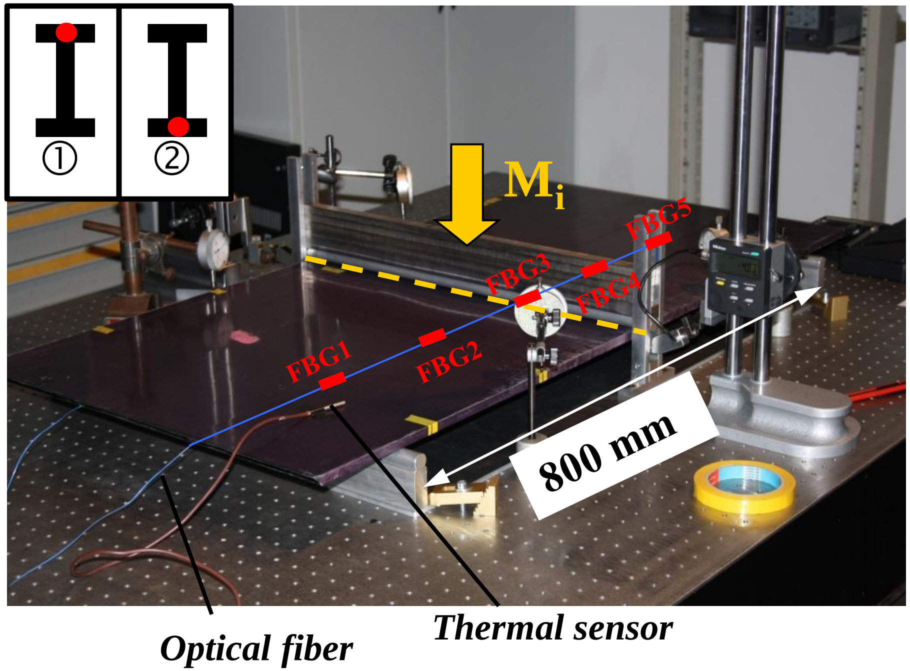

Procedure:

Measuring 3 defections (comparators) and 5 elongations ε (FBG) according to the load imposed (mass Mi)

Two case studies: FBG on top ① or on bottom ②

Si425 interrogator unit :

Main features: - acquisition of 250 Hz on 4 channels

- range: 1520 - 1570 nm (1 nm resolution)

Experimental results

Results for the case ① in 3 bending configuration:

Raw data of FBG (si425) in loading and unloading of the structure

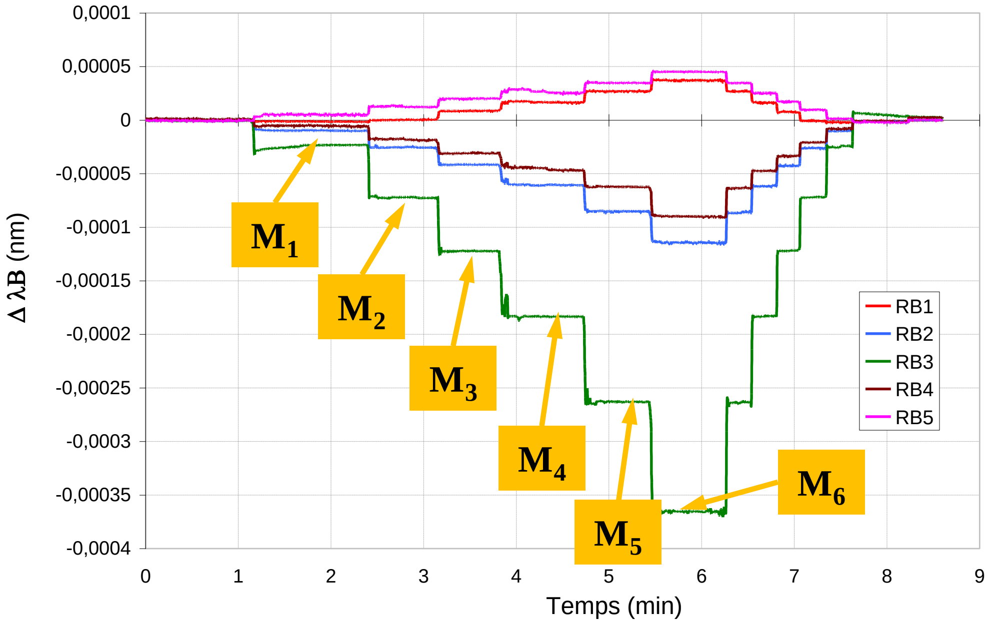

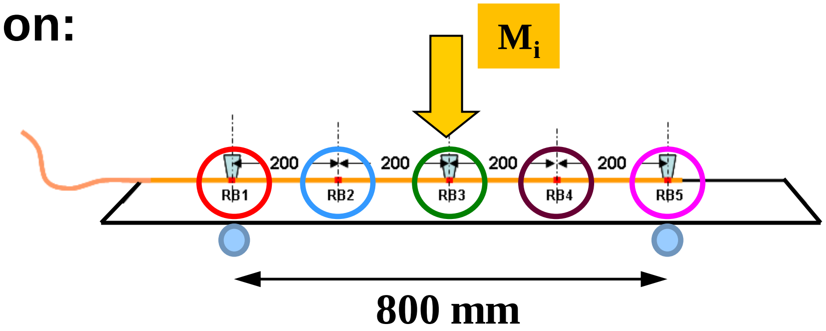

- Good sensitivity of FBGs
- Relatively symmetrical behaviour (errors due to the implementation of FBG?)
- Different behaviour of extremes:

$\Delta\lambda_B > 0$: tensile strain (FBG1 and FBG5)

$\Delta\lambda_B < 0$: compressive strain (FBG2, FBG3 and FBG4)

Values of deflection (FBG3)

	Poids (N)	Experimental deflection FBG3 (mm) *(standard deviation)*
M1	9,38	0,47 *(0,02)*
M2	26,35	1,22 *(0,02)*
M3	43,32	1,94 *(0,03)*
M4	61,64	2,76 *(0,05)*
M5	82,08	3,80 *(0,08)*
M6	102,53	5,05 *(0,12)*

Implementation of the model:

Model based on thin shells (SAMCEF)
Uniform mesh (mapping method)
Material: CC202/ET443 (composite 60%):
(properties with destructive tests of samples)

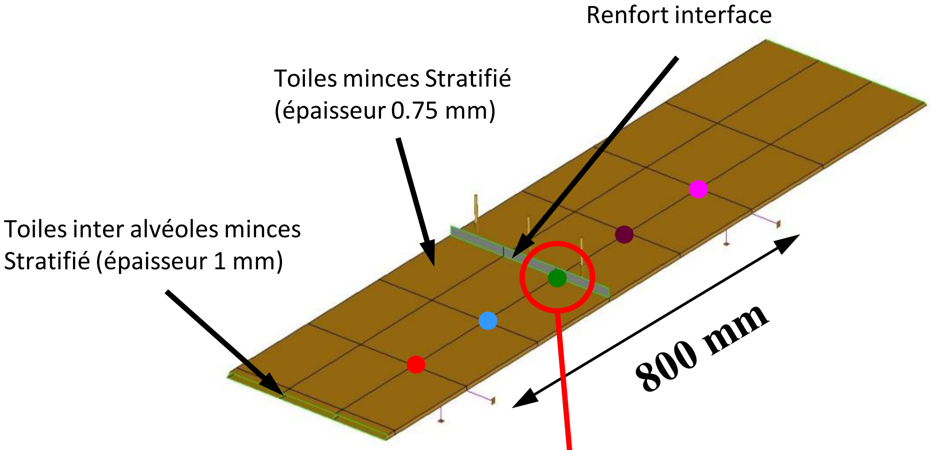

Correlation with exp deflection

Simulated results are obtained with a non-linear method (MECANO module) to take into account the cases M5&M6 where deflections are not smaller.

	Poids (N)	Flèche FBG3 expérimentale (mm) *(écart type)*	Flèche FBG3 simulée (mm)	Ecarts (%)
M1	9,38	0,47 *(0,02)*	0,43	8,5
M2	26,35	1,22 *(0,02)*	1,18	3,3
M3	43,32	1,94 *(0,03)*	1,94	0
M4	61,64	2,76 *(0,05)*	2,78	0,7
M5	82,08	3,80 *(0,08)*	3,79	1
M6	102,53	5,05 *(0,12)*	4,97	1,5

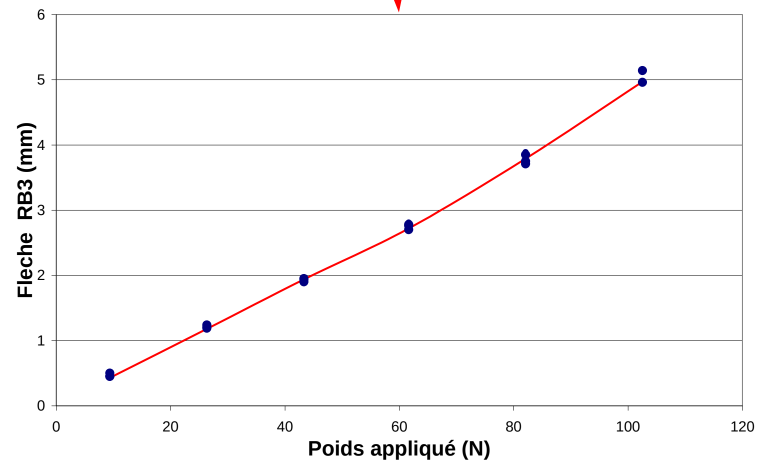

Vérification des paramètres du modèle en comparant la flèche FBG3 mesurée et simulée

Simulation results

Correlation with the experimental data (FBGs):

	Load (N)	ε_{yy} FBG1 (µm/m)		ε_{yy} FBG2 (µm/m)		ε_{yy} FBG3 (µm/m)		ε_{yy} FBG4 (µm/m)		ε_{yy} FBG5 (µm/m)	
		Exp.	Simu.	Exp.	Simu.	Exp.	Simu.	Exp.	Simu.	Exp.	Simu.
M1	9,38	-2,52	14	-12,6	-12,2	-29,86	-36,8	-7,41	-8,1	4,91	29
M2	26,35	0,84	27,8	-32,77	-30,6	-92,9	-100,7	-24,72	-26,5	15,55	42,51
M3	43,32	10,92	41,1	-53,78	-49,1	-156,77	-165,6	-39,55	-44,9	26,2	55,8
M4	61,64	21,01	55,4	-78,16	-69	-235,57	-237	-59,33	-64,8	31,11	70
M5	82,08	33,61	71,5	-109,26	-91,4	-336,77	-319,6	-79,93	-87,1	44,21	86,2
M6	102,53	48,74	87,4	-145,4	-117,7	-468,66	-413,7	-115,37	-112,8	58,13	102,2

Strain determination close to FBG location:

The tests are carried out at constant temperature
The exp. values obtained are calculated according to the equation:

$$\varepsilon_{yy} = b\frac{\Delta\lambda_b}{\lambda_b}$$

b~0,78 10-6 /µm/m

Hypothesis: FBGs give the longitudinal strain in the fiber ε_{yy} (reference of the model), corresponding to the scalar value of the second component of the strain tensor [11421 Code: composite strain tensor]

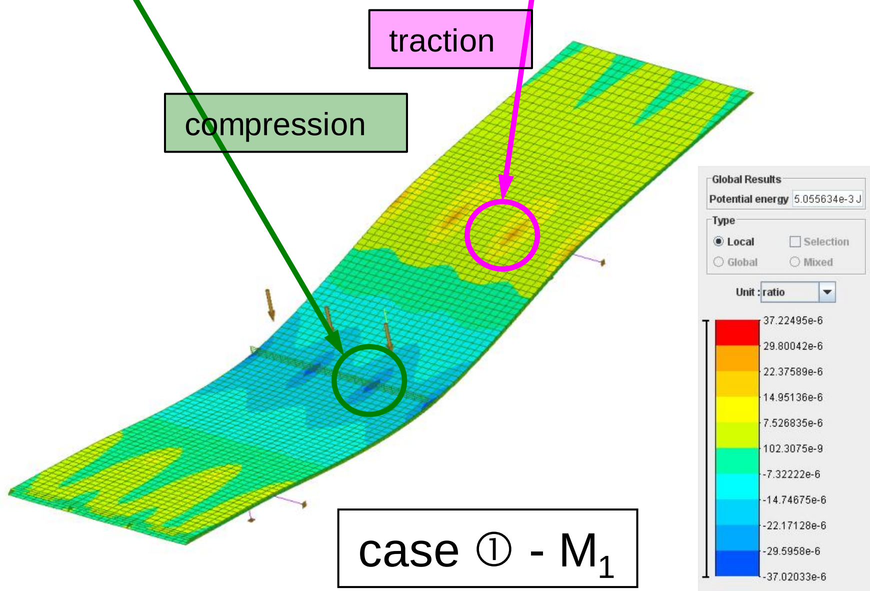

Conclusion: Feasibility

Use of FBGs is suitable for composite materials:

1) **Advantages:**

- Sensors embedded in the material
- Resistance to severe conditions of process
- Faculty to integrate OF between composite layers without significantly changing the mechanical properties of the laminate (concept: no-invasive)
- Sufficient sensitivity for our applications
- "Health matters": time tracking the behaviour of the composite (cracks, delaminations...)

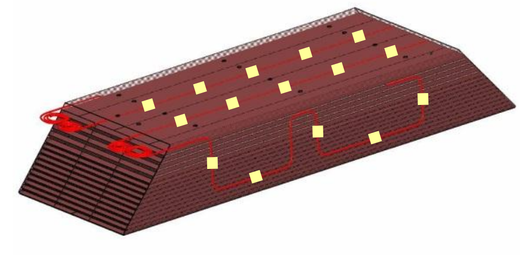

2) **Disadvantages:**

- Fragility of the zone of the FBG with possible rupture
- Delicate implementation and positioning errors
- Residual stress related conditions of the composite process
- High cost of the fiber (~ 1k€ with 5 FBGs) and interrogator unit (~ € 40k)

3) **Next Step:** **technological prototype** equipped with four optical fibers of 5 FBGs.

Integration of 4 Optical fibers for correlation : Tests / Simulations